

tyrosine kinases, including the Jak family kinases, and have failed to identify any such kinase in the complex. Our current model is that the activated gp130 receptor dimers recruit ErbB2 molecules to the complex, leading to ErbB2 clustering and kinase activation. It is difficult to rule out the transient participation of other molecule(s) in this process. Once ErbB2 is activated, the Shc/MAP kinase pathway will be activated, as well as ErbB3. The native ligands of the ErbB-family kinases are mostly peptide growth factors containing EGF-like repeats<sup>20</sup>. Recently, however, ErbB1/EGFR kinase was found to mediate signals of ultraviolet irradiation<sup>21</sup>, G proteins<sup>22</sup> and growth hormone<sup>23</sup>. Our data extend these observations and identify ErbB2 and ErbB3 as signal mediators of a cytokine. □

**Methods**

**Cell culture, transfection, selections and cell proliferation.** LNCaP, DU145 and CWR22 cells were maintained as described<sup>7</sup>. The cells were serum starved for 24 h followed by treatment with 200 ng ml<sup>-1</sup> IL-6 (UBI) for 30 min or the times indicated. The cDNA of scFv5R was subcloned into a mammalian expression vector, pcDNA3 (Invitrogen). LNCaP cells were transfected with this scFv5R construct by using LipofectAmine(Gibco BRL) following the manufacturer's instructions. The stable expression clones were obtained by selection for G418 resistance (600 µg ml<sup>-1</sup>) and further confirmed by the mobility shift of ErbB2 as described<sup>12</sup>. The cell proliferation assays (WST assays) were performed as described<sup>4</sup>.

**Immunoprecipitation, western blotting and in vitro kinase assays.** The immunoprecipitation and western blotting were performed following procedures described previously<sup>7</sup>. The autophosphorylation of ErbB2 and Tyk2 was assayed as described<sup>14,24</sup>. Briefly, the ErbB2 or Tyk2 immunoprecipitates were incubated in 20 mM HEPES, pH 7.4 with 10 mM MnCl<sub>2</sub> and 10 µCi [ $\gamma$ -<sup>32</sup>P]ATP for 10 min at room temperature. Reactions were stopped by adding an equal volume of 2 × SDS loading buffer and proteins resolved by SDS-PAGE, followed by autoradiography.

Received 23 December 1997; accepted 19 February 1998.

1. Hirano, T. The biology of interleukin-6. *Chem. Immunol.* **51**, 153–180 (1992).
2. Siegmund, M. J., Yamazaki, H. & Pastan, I. Interleukin 6 receptor mRNA in prostate carcinomas and benign prostate hyperplasia. *J. Urol.* **151**, 1396–1399 (1994).
3. Hutchins, D. & Steel, C. M. Regulation of ICAM-1 (CD54) expression in human breast cancer cell lines by interleukin 6 and fibroblast-derived factors. *Int. J. Cancer* **58**, 80–84 (1994).
4. Okamoto, M., Lee, C. & Oyasu, R. Interleukin-6 as a paracrine and autocrine growth factor in human prostatic carcinoma cells in vitro. *Cancer Res.* **57**, 141–146 (1997).
5. Myers, R. B., Srivastava, S., Oelschlager, D. K. & Grizzle, W. E. Expression of p160erbB-3 and p185erbB-2 in prostatic intraepithelial neoplasia and prostatic adenocarcinoma. *J. Nat. Cancer Inst.* **86**, 1140–1145 (1994).
6. Zhau, H. E. *et al.* Biomarkers associated with prostate cancer progression. *J. Cell. Biochem. (Suppl.)* **19**, 208–216 (1994).
7. Grasso, A., Wen, D., Pretlow, T. & Kung, H. ErbB kinases and NDF signaling in prostate cancer cells. *Oncogene* **15**, 2705–2717 (1997).
8. Holmes, W. E. *et al.* Identification of heregulin, a specific activator of p185erbB2. *Science* **256**, 1205–1210 (1992).
9. Wen, D. *et al.* Neu differentiation factor: a transmembrane glycoprotein containing an EGF domain and an immunoglobulin homology unit. *Cell* **69**, 559–572 (1992).
10. Dougall, W. C. *et al.* The neu-oncogene: signal transduction pathways, transformation mechanisms and evolving therapies. *Oncogene* **9**, 2109–2123 (1994).
11. Levitzki, A. & Gazit, A. Tyrosine kinase inhibition: an approach to drug development. *Science* **267**, 1782–1788 (1995).
12. Beerli, R. R., Wels, W. & Hynes, N. E. Intracellular expression of single chain antibodies reverts ErbB-2 transformation. *J. Biol. Chem.* **269**, 23931–23936 (1994).
13. Carraway, K. L. R. & Cantley, L. C. A new acquaintance for erbB3 and erbB4: a role for receptor heterodimerization in growth signaling. *Cell* **78**, 5–8 (1994).
14. Guy, P. M., Platko, J. V., Cantley, L. C., Cerione, R. A. & Carraway, K. L. R. Insect cell-expressed p180erbB3 possesses an impaired tyrosine kinase activity. *Proc. Natl. Acad. Sci. USA* **91**, 8132–8136 (1994).
15. Kishimoto, T., Taga, T. & Akira, S. Cytokine signal transduction. *Cell* **76**, 253–262 (1994).
16. Taniguchi, T. Cytokine signaling through nonreceptor protein tyrosine kinases. *Science* **268**, 251–255 (1995).
17. Chen-Kiang, S. Regulation of terminal differentiation of human B-cells by IL-6. *Curr. Topics Microbiol. Immunol.* **194**, 189–198 (1995).
18. Fukada, T. *et al.* Two signals are necessary for cell proliferation induced by a cytokine receptor gp130: involvement of STAT3 in anti-apoptosis. *Immunity* **5**, 449–460 (1996).
19. Siegall, C. B., Schwab, G., Nordan, R. P., FitzGerald, D. J. & Pastan, I. Expression of the interleukin 6 receptor and interleukin 6 in prostate carcinoma cells. *Cancer Res.* **50**, 7786–7788 (1990).
20. Carpenter, G. & Cohen, S. Epidermal growth factor. *J. Biol. Chem.* **265**, 7709–7712 (1990).
21. Rosette, C. & Karin, M. Ultraviolet light and osmotic stress: activation of the JNK cascade through multiple growth factor and cytokine receptors. *Science* **274**, 1194–1197 (1996).
22. Daub, H., Weiss, F. U., Wallasch, C. & Ullrich, A. Role of transactivation of the EGF receptor in signalling by G-protein-coupled receptors. *Nature* **379**, 557–560 (1996).
23. Yamauchi, T. *et al.* Tyrosine phosphorylation of the EGF receptor by the kinase Jak2 is induced by growth hormone. *Nature* **390**, 91–96 (1997).
24. Rui, H., Kirken, R. A. & Farrar, W. L. Activation of receptor-associated tyrosine kinase JAK2 by prolactin. *J. Biol. Chem.* **269**, 5364–5368 (1994).

**Acknowledgements.** We thank N. E. Hynes for the scFv5R clone, J. Jacobberger and T. G. Pretlow for CWR22 cells, and A. W. Grasso and K. Everiss for reading the manuscript. This work was supported by NIH grants. Y.Q. is a recipient of an NCI research oncology training fellowship.

Correspondence and requests for materials should be addressed to H.J.K. (e-mail: hxk5@po.cwru.edu).

## Receptor clustering as a cellular mechanism to control sensitivity

Dennis Bray, Matthew D. Levin & Carl J. Morton-Firth

Department of Zoology, University of Cambridge, Downing Street, Cambridge CB2 3EJ, UK

Chemotactic bacteria such as *Escherichia coli* can detect and respond to extremely low concentrations of attractants, concentrations of less than 5 nM in the case of aspartate<sup>1</sup>. They also sense gradients of attractants extending over five orders of magnitude in concentration (up to 1 mM aspartate)<sup>2,3</sup>. Here we consider the possibility that this combination of sensitivity and range of response depends on the clustering of chemotactic receptors on the surface of the bacterium<sup>4</sup>. We examine what will happen if ligand binding changes the activity of a receptor, propagating this change in activity to neighbouring receptors in a cluster<sup>5,6</sup>. Calculations based on these assumptions show that sensitivity to extracellular ligands increases with the extent of spread of activity through an array of receptors, but that the range of concentrations over which the array works is severely diminished. However, a combination of low threshold of response and wide dynamic range can be attained if the cell has both clusters and single receptors on its surface, particularly if the extent of activity spread can adapt to external conditions. A mechanism of this kind can account quantitatively for the sensitivity and response range of *E. coli* to aspartate.

The effects of activity spread may be illustrated by considering

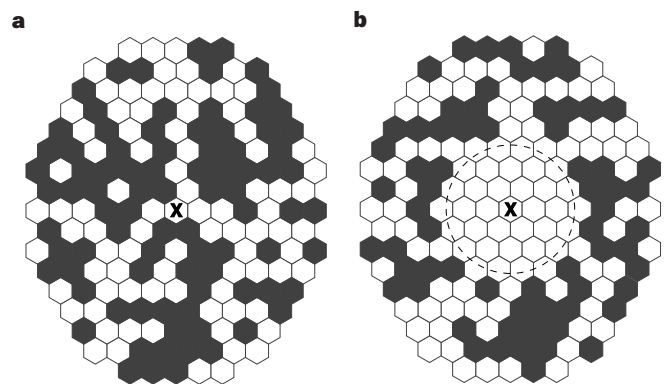


**Figure 1** Activity spread in a cluster of receptors. Part of a hypothetical 1,000-receptor array is shown; individual receptor molecules are represented as white or grey hexagons, depending on their conformation. Receptors are supposed to switch randomly between a high-activity conformation (grey) and a low-activity conformation (white). **a**, One receptor in the centre of the array, marked with a cross, is occupied by a ligand molecule and consequently is in the low-activity conformation. **b**, In this array the ligand-bound, low-activity state of the central receptor has spread to 36 neighbouring unoccupied receptors. Because of this 'infectivity', the single ligand molecule produces a larger change in the array and the signal sent from the array is stronger. However, the range over which the array detects changes in the concentration of ligand is much smaller in **b** than in **a**.

a model array of 1,000 receptors with properties loosely based on the chemotactic receptors of coliform bacteria<sup>7,8</sup>. Each receptor is assumed to adopt either an active or an inactive conformation and to switch rapidly between the two on a submillisecond timescale. In its active conformation, a receptor signals to downstream elements of the pathway. The probability of occupying this conformation constitutes the 'activity' of the receptor. We will denote this activity by the symbol  $p$ , using  $p_0$  for the activity of a receptor not occupied by ligand and  $p_1$  for the activity of a receptor occupied by ligand. We will consider below the possibility that, because of cooperative interactions, unoccupied receptors can also adopt a probability  $p_1$ . Both  $p_0$  and  $p_1$  can change with adaptation, but we will assume that  $p_0$  is always greater than  $p_1$  so that ligand binding causes a decrease in activity, as it does in bacterial chemotaxis.

In the initial array of 'naive' receptors, let  $p_0 = 0.5$ ; that is, we assume that roughly half of the receptors in the array are active at any time (Fig. 1a). The total activity of the array—the strength of the signal it sends to downstream elements of the signal pathway—will then be  $Np_0 = 500$  units (each 'unit' being the strength of signal produced by one receptor in its active conformation). If we now expose the array to molecules of ligand A, then some of these molecules ( $n_A$ ) will bind to individual receptors. The occupied receptors will reduce their probability of switching to an active state to  $p_1$  and the total activity of the array will become smaller ( $n_A p_1 + (N - n_A) p_0$ ). Thus, if 200 molecules of ligand A bind and if, with each binding, a receptor reduces its activity from 0.5 to zero ( $p_1 = 0$ ), then the total output will decrease from 500 to 400 ( $200 \times 0.0 + 800 \times 0.5$ ) units.

In this example, the change in total activity is given by the number of receptors that are newly bound to ligand A, multiplied by the change in activity per receptor. However, if each molecule A that binds to the array affects the switching probability of multiple contiguous receptors, then the same number of binding events will generate a larger change in activity (Fig. 1b). Specifically, if we assume that a single binding event 'infects'  $n_i$  receptors (changes their probability of being active from  $p_0$  to  $p_1$ ), then the change in output activity  $\Delta P$  will be (for low concentrations of ligand)  $\Delta P = n_A n_i \sigma$ , where  $n_A$  is the number of ligand molecules bound and  $\sigma (= p_0 - p_1)$  is the change in activity per receptor.

For an array of  $N$  receptors, each with a single binding site of dissociation constant  $K_d$  exposed to ligand A at a concentration  $C_A$ ,  $n_A/N = C_A/(C_A + K_d)$ . As the concentration of A becomes less, the change in activity will fall until it reaches a minimum detectable by experimental observation. Calling this minimum concentration  $C_A^{\min}$  and observing that  $n_A^{\min} = \Delta P^{\min}/n_i \sigma$ , then:

$$C_A^{\min} = \left( \frac{n_A^{\min}}{N - n_A^{\min}} \right) K_d = \left( \frac{\Delta P^{\min}/n_i \sigma}{N - \Delta P^{\min}/n_i \sigma} \right) K_d \quad (1)$$

From equation (1) we see that the minimum detectable concentration of ligand (the threshold concentration) decreases as the extent of activity spread grows larger. Indeed, if  $n_i$  is sufficiently large, then the entire array can switch state in response to the binding of a single ligand molecule. But if a single binding event fires the whole array, then the system will be unable to detect binding of subsequent ligand molecules. As this extreme example illustrates, the larger  $n_i$  is, the lower the range over which detection can occur.

To calculate the maximum detectable concentration of ligand, we must consider adaptation. The sensory systems of single cells, like those of entire organisms, adjust to ambient conditions by continually changing their baseline activity. This enables them to react to small changes even against a high background level of stimulation. The most effective form of adaptation (capable of extending over the widest range) occurs if the activity always returns to its original value—that is, it is exact<sup>9</sup>.

Applying exact adaptation, we see that, following exposure to ligand, the probabilities that receptors will be in the active conformation ( $p_0$  and  $p_1$ ) must rise so as to restore the original activity

(500 units in our example). We cannot say exactly how the probabilities will change but there are boundary conditions. Thus, if  $p_1$  remains zero,  $p_0 = 1$  and  $n_i = 1$ , then an output value of 500 units will be reached when just half of the receptors are occupied ( $500 \times 1 + 500 \times 0$ ). This will occur when the ambient concentration of ligand equals the  $K_d$  of the receptors, which is a very poor performance. It becomes even worse if  $p_0 < 1$  or  $n_i > 1$ .

A much wider range can be obtained by allowing both  $p_0$  and  $p_1$  to rise with increasing ligand concentration, subject to the constraint that the total activity of the array must be 500 units. That is,  $(1,000 - n_A)p_0 + n_A p_1 = 500$ . The widest possible range is reached by making  $p_0 = 1$ , and allowing  $p_1$  to rise as close as possible to 0.5; then the total activity of the array will be close to 500 even when all receptors are occupied ( $1,000 \times 0.5 = 500$ ). In practical terms, the upper limit in concentration of ligand will occur when the output activity is so close to 500 that the difference cannot be measured experimentally, that is, when addition of saturating levels of ligand A raises the activity by less than  $\Delta P^{\min}$ .

We must therefore calculate how many molecules of ligand A must bind to our array before the output activity comes within

### Box 1 Raindrops calculation

Consider an array of  $N$  membrane-bound receptors (represented by the grey area in the figure). Let some of these receptors bind to ligand A and let each binding event change the average activity of  $n_i$  receptors (white circles in the figure). What is the probability that any given receptor of the initial set of  $N$  remains unaffected after  $n_A$  ligand molecules have bound?

If one ligand molecule binds, then  $n_i$  receptors will change their activity. The probability that a given receptor is not affected by this event is given by the ratio:

$$\frac{N - n_i}{N} = \left( 1 - \frac{n_i}{N} \right)$$

A second ligand molecule has available to it  $N - 1$  sites (as one is already occupied). The number of receptor molecules changing their conformation in response to this second binding is again  $n_i$ , so that the probability that any given receptor is not affected by the second ligand is:

$$\frac{N - 1 - n_i}{N - 1} = \left( 1 - \frac{n_i}{N - 1} \right)$$

These two ligand binding events are independent. Therefore, the probability that a given receptor will not be affected by either binding event is the product of the two, namely:

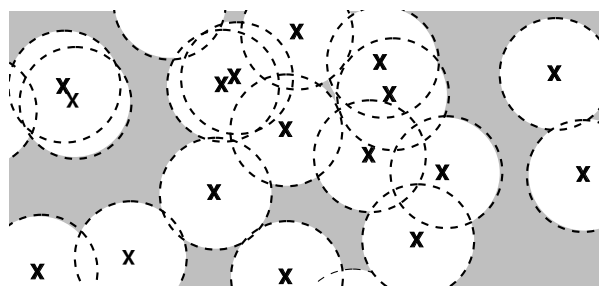
$$\left( 1 - \frac{n_i}{N} \right) \left( 1 - \frac{n_i}{N - 1} \right)$$

The same argument holds for each successive molecule of ligand A, so that the probability of being unaffected after  $n_A$  ligand molecules have bound is:

$$\left( 1 - \frac{n_i}{N} \right) \left( 1 - \frac{n_i}{N - 1} \right) \left( 1 - \frac{n_i}{N - 2} \right) \dots \left( 1 - \frac{n_i}{N - n_A + 1} \right)$$

The number of ligand molecules unaffected by the binding of  $n_A$  receptor molecules is given by the function  $R$ , where:

$$R = N \prod_{k=1}^{n_A} \left( 1 - \frac{n_i}{N - k + 1} \right)$$



$\Delta P^{\min}$  of maximum. Again we include the possibility of activity spread, but in this case we must allow for overlap between successive receptor bindings (the raindrop effect; see Box 1). The number of ligand molecules required can be deduced from the relationship  $\Delta P^{\min}/\sigma \leq R$ , where function  $R(N, n_i, n_A)$  is the number of receptors remaining unaffected after  $n_A$  molecules of ligand have bound (see Box 1) and  $\sigma (= p_0 - p_1)$  has its optimal value of 0.5. The value of  $R$  can be readily computed for increasing values of  $n_A$  until the above inequality is satisfied. This gives  $n_A^{\max}$ , from which we deduce the maximum detectable concentration of ligand  $C_A^{\max}$ :

$$C_A^{\max} = \left( \frac{n_A^{\max}}{N - n_A^{\max}} \right) K_d \quad (2)$$

We thus have equations for the minimum and maximum ligand concentrations for a range of activity spreads (that is,  $n_i$  values) and for different levels of detectable activity  $\Delta P^{\min}$ . As seen in Fig. 2, the minimum concentration calculated from equation (1) falls in hyperbolic fashion with increasing  $n_i$ , an increase from  $n_i = 1$  to  $n_i = 2$  producing a twofold decrease in  $C_A^{\min}$ . However, the maximum concentration calculated from equation (2) falls very much more steeply. Here an increase from  $n_i = 1$  to  $n_i = 2$  produces a

greater than 20-fold drop in the maximum (saturating) concentration of ligand A. Thus, activity spread lowers the threshold but severely restricts the dynamic range over which the receptor array can operate.

Let us now apply these ideas to bacterial chemotaxis and in particular to the system by which *E. coli* detect and swim towards distant sources of aspartate. Each cell has ~2,000 dimeric aspartate receptors on its surface, many of them clustered into a patch at the polar regions of the cell<sup>4,10,11</sup>. The receptors are part of a complex of proteins, including the autophosphorylating kinase CheA, which transfers phosphoryl groups onto CheY<sup>12</sup>. Phosphorylated CheY (CheYp) molecules diffuse to the flagellar motors, causing them to rotate in a clockwise direction and thereby producing a random change in direction of the bacterium<sup>13</sup>. The rate at which phosphate groups are generated by the receptor complex falls when aspartate is bound<sup>14</sup>, causing the motors to turn anticlockwise and the cell to persist in its current direction. In effect, the flux of phosphoryl groups from the receptor complex constitutes its output activity, equivalent to the array activity  $P$  mentioned above.

Much quantitative information is available relating to the biochemical steps of this chemotactic signal pathway<sup>7</sup>. In particular, the rates of phosphotransfer from the receptor complex to CheY and the rate of loss of phosphate groups from CheYp (mainly through CheZ) are known<sup>15,16</sup>. We also have estimates of the relation between the steady-state concentration of CheYp and the flagellar rotation bias (the time spent in a smooth swimming mode)<sup>17</sup>. These experimentally measured values allow us to estimate the (hypothetical) switching frequency of aspartate receptors corresponding to different swimming biases (Table 1).

The values in Table 1 give an estimate of the change in output activity,  $\Delta P^{\min}$ , needed to produce a bias change of 0.1, which is the smallest detectable value for tethered bacteria. With  $\Delta P^{\min}$  we can calculate the smallest number of receptors that must change their average activity from 0.048 (the resting value) to zero, and hence the smallest concentration of aspartate that can be detected. In the absence of activity spread, this value is about 0.22  $\mu\text{M}$  or 220 nM, a value close to that given by computer models of the chemotaxis pathway on the basis of experimentally determined rates and concentrations in the chemotaxis pathway<sup>18,19</sup>.

However, the actual threshold of the chemotactic system is much lower than indicated by this figure. Classic experiments in which *E. coli* cells tethered to a coverslip were exposed to small quantities of chemoattractant delivered iontophoretically indicated that a change in receptor occupancy of as little as 1/600 could produce a detectable change in swimming behaviour<sup>1</sup>. With a  $K_d$  of 1  $\mu\text{M}$ <sup>20,21</sup>, this change corresponds to a minimum detectable concentration of about 2 nM aspartate. Estimates obtained using caged aspartate<sup>22</sup> also show a response threshold corresponding to about 0.002 occupancy, or ~2 nM (R. Jasuja and S. Khan, manuscript in preparation). Another difficulty with current models of the chemotaxis pathway concerns the response to substances such as ribose that are detected by receptors present in small numbers. The ribose receptor, Trg, accounts for only ~1% of the total chemotactic receptors of the cell and yet operates through the same phosphorylation cascade as the aspartate receptors<sup>23</sup>. On a simple 'head-count' mechanism, signals from Trg receptors would simply not be heard.

Both discrepancies between theory and experiment can be resolved if activities can spread from one receptor to its neighbours in the cluster. Using the equations already given, we can readily achieve the required threshold to both aspartate or ribose, given sufficient activity spread. But, as before, we must also consider the range of detection, which become less as the infectivity grows. Information on the upper limits of chemotactic detection is difficult to find: the best estimates are probably those obtained using a capillary accumulation assay<sup>2</sup>. For the non-hydrolysable analogue of aspartate,  $\alpha$ -methylaspartate, concentrations in the range from 0.3  $\mu\text{M}$  to 0.1 M produced chemotactic responses. As the binding

**Table 1** Receptor activity level calculated from swimming performance

Rotational bias	CheYp ( $\mu\text{M}$ )	Output activity ( $P$ )	Receptor activity
0	15	2,000	1.0
0.75	2.8	109	0.054
0.85	2.5	95	0.048
0.95	2.0	74	0.037
1.0	0	0	0

The rotational bias of an *E. coli* cell is the fraction of time the flagellum spends in a smooth-swimming (or anticlockwise motor rotation) mode. The bias of a wild-type cell without chemotactic stimulation is about 0.85 (refs 1, 19). Bias is controlled by the cytoplasmic concentration of CheYp and there is a cooperative relationship between the two, with a Hill coefficient of 5–6 (ref. 17). Here we use a relationship of the form<sup>18</sup>  $\text{bias} = 1 - Y_p^{5.5} / (5.67(2.51)^{5.5} + Y_p^{5.5})$ , in which the steady-state concentration of CheYp ( $Y_p$ ) in a wild-type, unstimulated cell is 2.51  $\mu\text{M}$ . We take the lower limit of  $Y_p$  to be zero and the upper limit to be the concentration at which the bias falls below 0.001, namely 15  $\mu\text{M}$ . In a wild-type cell, the concentration of CheYp depends mainly on the rate of formation of CheYp by the receptor complex and the rate of breakdown of CheYp by CheZ. At steady state, these two balance, so that  $P(20 - Y_p) \propto ZY_p$ , where  $P$  is the output activity of the chemotactic receptors (as defined above),  $Z$  is the activity of CheZ, and the total concentration of CheY is taken to be 20  $\mu\text{M}$  (ref. 27). This leads to a relationship of the form  $P = \text{const}(Y_p / (20 - Y_p))$ , and we assign the constant a value of 2,000/3 so that  $P = 2,000$  at  $Y_p = 15 \mu\text{M}$  (bias of 0.001, receptors fully active) and  $P = 0$  at  $Y_p = 0.0 \mu\text{M}$  (bias of 1.0, receptors inactive). The average activity of individual receptors is then calculated as  $P/2,000$ .

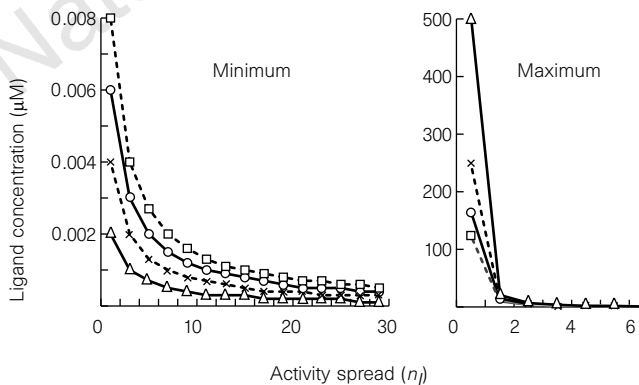


**Figure 2** Changes in the response to threshold and range of ligand concentration with the extent of activity spread. Minimum and maximum ligand concentrations to which the model 1,000-receptor array can respond, with output values of 500 units, are plotted against activity spread ( $n_i$ ). In each graph, four different values of the minimum detectable change in output activity ( $\Delta P^{\min}$ ) are shown as follows: one unit, triangles connected by complete lines; two units, crosses connected by dashed lines; three units, circles connected by complete lines; and four units, squares connected by dashed lines. Note the differences in scale of the two graphs.

**Table 2 Effect of receptor clustering on chemotactic threshold and range**

No. of receptors free	No. of receptors clustered	Activity spread ( $n_i$ )	Minimum conc. ( $\mu\text{M}$ )	Maximum conc. ( $\mu\text{M}$ )
2,000	0	1	0.22	730
1,000	1,000	1	0.22	730
1,000	1,000	10	0.038*	360†
1,000	1,000	100	0.004*	360†
0	2,000	1	0.22	730
0	2,000	10	0.019	4.2
0	2,000	100	0.002	0.33

Experimental data on the chemotaxis of *E. coli* were used with equations (1) and (2) to estimate the minimum and maximum detectable concentrations of aspartate. The minimum detectable concentration of aspartate,  $C^{\text{min}}$  (also referred to as the threshold), was calculated from equation (1) using a  $K_d$  of 1  $\mu\text{M}$  for a non-adapted aspartate receptor, a value of  $\Delta P^{\text{min}} = 17.5$  obtained from the data in Table 1, and a change in activity associated with individual receptors of  $\sigma = 1 - 0.048 = 0.95$ . The maximum detectable concentration of aspartate,  $C^{\text{max}}$  (also referred to as the saturating concentration, or chemotactic range), was calculated using a  $K_d$  for the binding of aspartate to the fully methylated (fully adapted) chemotactic receptor of 7  $\mu\text{M}$  (refs 24, 25) and values of R calculated as described in Box 1. \* Contribution from free receptors assumed to be negligible. † Contribution from clustered receptors assumed to be negligible.

of methylaspartate to the aspartate receptor is relatively weak ( $K_d$  close to 0.1 mM), we estimate that aspartate itself (which has a  $K_d$  of 1  $\mu\text{M}$ ) should give the same change in receptor occupancy in the range of 3 nM to 1 mM.

In Table 2 we give the expected minimum and maximum concentrations of aspartate detected by a set of 2,000 aspartate receptors, making different assumptions about their degree of clustering and activity spread. These values also include an increase in the  $K_d$  for aspartate with adaptation<sup>24,25</sup>. We see that if half of the receptors are freely diffusing and the other half are clustered and show an infectivity of 100, aspartate will be detected in the concentration range 4 nM to 360  $\mu\text{M}$ . However, the best overall performance is achieved if receptors are totally aggregated at low concentrations of aspartate and totally non-aggregated at high concentrations. In this case, the cell can achieve a range of detection at concentrations from 2 nM to 730  $\mu\text{M}$ , a range of greater than five orders of magnitude and similar to the best estimates of the actual performance. Changes of this kind might be produced, for example, by the methylating enzyme CheR which can link adjacent receptors and whose binding is reduced by methylation<sup>11,26</sup>.

The model we have proposed requires that when chemotactic receptors cluster on the cell surface, the activity of one receptor influences that of its neighbours. Furthermore, to obtain a combination of sensitivity and range of response the cell must be able to control either the aggregation itself or the degree to which the receptor activity can propagate. We predict, for example, that aggregation (or activity spread) will be lowest when the cell has adapted to high concentrations of ambient attractant. We also expect that chemoattractants such as ribose that operate through minor receptors will saturate at very low concentrations (as they can be sensed only through activity spread). There should be conditions in which the degree of aggregation, and hence the sensitivity to chemoattractants, is impaired (this might occur, for example, in mutants lacking CheR and CheB). Finally, given the simplicity of this mechanism, we anticipate that it will be widely used by cells other than bacteria and for purposes other than chemotaxis. □

Received 12 January; accepted 26 February 1998.

- Segall, J. E., Block, S. M. & Berg, H. C. Temporal comparisons in bacterial chemotaxis. *Proc. Natl Acad. Sci. USA* **83**, 8987–8991 (1986).
- Mesibov, R., Ordal, G. W. & Adler, J. The range of attractant concentrations for bacterial chemotaxis and the threshold and size of response over this range. Weber law and related phenomena. *J. Gen. Physiol.* **62**, 203–223 (1973).
- Berg, H. C. & Tedesco, P. M. Transient response to chemotactic stimuli in *Escherichia coli*. *Proc. Natl Acad. Sci. USA* **72**, 3235–3239 (1975).
- Maddock, J. R. & Shapiro, L. Polar location of the chemoreceptor complex in the *Escherichia coli* cell. *Science* **259**, 1717–1723 (1993).
- Gardina, P. J. & Manson, M. D. Attractant signaling by an aspartate chemoreceptor dimer with a single cytoplasmic domain. *Science* **274**, 425–426 (1996).
- Parkinson, J. S. & Blair, D. F. Does *E. coli* have a nose? *Science* **259**, 1701–1702 (1993).
- Stock, J. B. & Surette, M. G. In *Escherichia and Salmonella: Cellular and Molecular Biology* (ed. Neidhardt, F. C.) 1103–1129 (Am. Soc. Microbiol., Washington DC, 1996).
- Eisenbach, M. Control of bacterial chemotaxis. *Mol. Microbiol.* **4**, 161–167 (1996).

- Barkai, N. & Leibler, S. Robustness in simple biochemical networks. *Nature* **387**, 913–917 (1997).
- Gegner, J. A., Graham, D. R., Roth, A. F. & Dahlquist, F. W. Assembly of an MPC receptor, CheW, and kinase CheA complex in the bacterial chemotaxis signal transduction pathway. *Cell* **70**, 975–982 (1992).
- Li, J. Y., Li, G. Y. & Weis, R. M. The serine chemoreceptor from *Escherichia coli* is methylated through an interdimer process. *Biochemistry* **36**, 11851–11857 (1997).
- Schuster, S. C., Swanson, R. V., Alex, L. A., Bourret, R. B. & Simon, M. I. Assembly and function of a quaternary signal transduction complex monitored by surface plasmon resonance. *Nature* **365**, 343–346 (1993).
- Barak, R. & Eisenbach, M. Correlation between phosphorylation of the chemotaxis protein CheY and its activity at the flagellar motor. *Biochemistry* **31**, 1821–1826 (1992).
- Ninfa, E. G., Stock, A., Mowbray, S. & Stock, J. Reconstitution of the bacterial chemotaxis signal transduction system from purified components. *J. Biol. Chem.* **266**, 9764–9770 (1991).
- Stewart, R. C. Activating and inhibitory mutations in the regulatory domain of CheB, the methyltransferase in bacterial chemotaxis. *J. Biol. Chem.* **266**, 1921–1930 (1993).
- Lukat, G. S., McCleary, W. R., Stock, A. M. & Stock, J. B. Phosphorylation of bacterial response regulator proteins by low molecular weight phospho-donors. *Proc. Natl Acad. Sci. USA* **89**, 718–722 (1992).
- Kuo, S. C. & Koshland, D. E. Jr Multiple kinetic states for the flagellar motor switch. *J. Bacteriol.* **171**, 6279–6287 (1989).
- Bray, D., Bourret, R. B. & Simon, M. I. Computer simulation of the phosphorylation cascade controlling bacterial chemotaxis. *Mol. Biol. Cell* **4**, 469–482 (1993).
- Levin, M. D., Morton-Firth, C. J., Abouhamad, W. N., Bourret, R. B. & Bray, D. Origins of individual swimming behavior in bacteria. *Biophys. J.* **74**, 175–181 (1998).
- Biemann, H.-P. & Koshland, D. E. Aspartate receptors of *Escherichia coli* and *Salmonella typhimurium* bind ligand with negative and half-of-sites cooperativity. *Biochemistry* **33**, 629–634 (1994).
- Aksamit, R. R., Howlett, B. J. & Koshland, D. E. Jr Soluble and membrane-bound aspartate-binding activities in *Salmonella typhimurium*. *J. Bacteriol.* **123**, 1000–1005 (1975).
- Khan, S. et al. Excitatory signaling in bacteria probed by caged chemoeffectors. *Biophys. J.* **65**, 2368–2382 (1993).
- Hazelbauer, G. L., Engstrom, P. & Harayama, S. Methyl-accepting chemotaxis protein III and transducer gene *trg*. *J. Bacteriol.* **145**, 43–49 (1981).
- Borkovich, K. A., Alex, L. A. & Simon, M. I. Attenuation of sensory receptor signaling by covalent modification. *Proc. Natl Acad. Sci. USA* **89**, 6756–6760 (1992).
- Yonekawa, H. & Hayashi, H. Desensitization by covalent modification of the chemoreceptor of *Escherichia coli*. *FEBS Lett.* **198**, 21–24 (1986).
- Wu, J., Li, J., Li, G., Long, D. G. & Weis, R. M. The receptor binding site for the methyltransferase of bacterial chemotaxis is distinct from the sites of methylation. *Biochemistry* **35**, 4984–4993 (1996).
- Stock, A. M., Koshland, D. E. Jr & Stock, J. B. Homologies between the *Salmonella typhimurium* CheY protein and proteins involved in the regulation of chemotaxis, membrane protein synthesis, and sporulation. *Proc. Natl Acad. Sci. USA* **82**, 7989–7993 (1985).

**Acknowledgements.** We thank M. Keeling for help with mathematics, S. Khan for permission to cite unpublished data, and R. Bourret, E. Siggia and T. Lamb for criticisms of the manuscript.

Correspondence and requests for materials should be addressed to D.B. (e-mail: d.bray@zoo.cam.ac.uk).

## Chromatin remodelling by the glucocorticoid receptor requires the BRG1 complex

Christy J. Fryer & Trevor K. Archer

Departments of Obstetrics & Gynaecology, Biochemistry and Oncology, University of Western Ontario, London Regional Cancer Centre, 790 Commissioners Rd East, London, Ontario N6A 4L6, Canada

The assembly of transcriptional regulatory DNA sequences into chromatin plays a fundamental role in modulating gene expression<sup>1,2</sup>. The promoter of the mouse mammary-tumour virus (MMTV) is packaged into a regular array of nucleosomes when it becomes stably integrated into mammalian chromosomes, and has been used to investigate the relationship between chromatin architecture and transcriptional activation by the hormone-bound glucocorticoid and progesterone receptors<sup>3,4</sup>. In mammalian cells that express both of these receptors, the progesterone receptor activates transcription from transiently transfected MMTV DNA<sup>5,6</sup> but not from organized chromatin templates<sup>7</sup>. Moreover, the activated progesterone receptor inhibits the chromatin remodelling and consequent transcriptional stimulation that is mediated by the glucocorticoid receptor. Here we investigate the mechanism of this inhibition by characterizing the interaction of the glucocorticoid receptor with transcriptional co-activator and chromatin remodelling protein complexes<sup>2,8</sup>. We show that when this receptor is prevented from interacting with the hBRG1/BAF chromatin remodelling complex, it can activate transcription from transiently transfected